

Search for brightness fluctuations in the zodiacal light at 25 μm with ISO^{*}

Péter Ábrahám^{1,2}, Christoph Leinert¹, and Dietrich Lemke¹

¹ Max-Planck-Institut für Astronomie, Königstuhl 17, D-69117 Heidelberg, Germany

² Konkoly Observatory of the Hungarian Academy of Sciences, P.O.Box 67, H-1525 Budapest, Hungary

Received 16 April 1997 / Accepted 5 August 1997

Abstract. We mapped at 25 μm five $\approx 0.5^\circ \times 0.5^\circ$ fields at low, intermediate and high ecliptic latitude with the photometer on-board the Infrared Space Observatory. The goal was to search for potential structures in the zodiacal light. No structures were seen in these five sample fields. For an aperture of 3' diameter we find an upper limit for the underlying rms brightness fluctuations of $\pm 0.2\%$, which corresponds at high ecliptic latitudes to ± 0.04 MJy/sr or ± 25 mJy in the beam.

Key words: interplanetary medium – infrared: solar system – diffuse radiation

1. Introduction

One of the main characteristics of the zodiacal light is the large-scale smoothness of its brightness distribution over the sky. Variability due to Thompson scattering of solar radiation at interplanetary plasma clouds is usually a small effect, related to high solar activity, even at visual wavelengths (Richter et al. 1982). The high incidence of localised brightness structures, observed by Lévassieur and Blamont (1973) from the satellite D2A at 653 nm and attributed by them to meteor streams, is not typical for the zodiacal light in general. However, two types of elongated structures detected by the infrared satellite IRAS are now considered as typical phenomena: the asteroidal bands and the cometary trails. The asteroidal bands are located at low ecliptic latitudes, $|\beta| \leq 12^\circ$, have a brightness enhancement of several percent of the zodiacal light and a width of two to four degrees (see, e.g. Reach 1992). They are thought to result from debris created in collisions between members of asteroid families (e.g. Sykes 1990). The cometary dust trails are fainter and narrower, having a peak brightness of about 1% of the zodiacal light and

a width of one or a few arcminutes (Sykes and Walker 1992). They are due mainly to mm-sized dust particles released from the comet at lower velocities than the particles constituting the tail and which therefore concentrate in the comet orbital plane.

Little is known on the graininess of zodiacal light brightness at small spatial scales. It has to exist at some level since the zodiacal light is produced from particles which are replenished from localised sources, comets and asteroids. Depending on amplitude and scale of such fluctuations, the sensitivity of deep source counts and the usefulness of fluctuation analysis to recover the flux distribution of still fainter sources may be reduced. This may adversely affect some of the extragalactic studies to be performed with infrared satellites.

Therefore, as part of the ISOPHOT guaranteed time programme on infrared diffuse sky brightness, we mapped a few fields of $\approx 0.5^\circ \times 0.5^\circ$ at 25 μm in order to look for fluctuations in the zodiacal light at low, intermediate and high ecliptic latitudes. These fields were selected for low cirrus emission and avoided any brighter infrared point sources. Since in the wavelength range of 7 μm to 60 μm the zodiacal light is at its maximum, any detected fluctuation probably would be due to the zodiacal light.

2. Observations and data reduction

Five fields in low cirrus regions were mapped in raster mode (called 'AOT P22') with 3' stepsize using the ISOPHOT P_25 filter and 180'' aperture (Lemke et al. 1996). Central positions of the fields and sizes of the maps are listed in Table 1. M01, M02, M03 refer to low background positions at ecliptic latitudes of $\beta = 87^\circ, 74^\circ, 67^\circ$, respectively. NGP stands for a field near the North Galactic Pole and ECL90,0 for a field in the ecliptic plane to be observed when the distance from the Sun is about 90° .

Data reduction was performed using the ISOPHOT Interactive Analysis (PIA) version 6.0, including correction for non-linearities of the electronics, subtraction of dark current, and removal of cosmic ray hits (in some measurements the latter was performed by visual inspection of the integration ramps). The data were calibrated by using the default responsivity of 0.46

Send offprint requests to: Peter Abraham

* Based on observations with ISO, an ESA project with instruments funded by ESA member states (especially the P/I countries France, Germany, the Netherlands and the United Kingdom) with participation of ISAS and NASA.

Table 1. Coordinates and sizes of the mapped fields

Field Name	J2000		Ecliptic coordinates			Size of the map
	α	δ	longitude	latitude	$\lambda - \lambda_{\odot}$	
M01	17h50m14s	+69d41'14''	105.09°	+86.74°	-161.2°	27' x 27'
M02	15h00m33s	+70d43'12''	145.39°	+73.56°	-108.6°	27' x 27'
M03	13h36m12s	+70d34'53''	140.38°	+66.81°	-78.5°	27' x 27'
NGP	13h42m32s	+40d29'13''	183.58°	+46.60°	+98.4°	45' x 45'
ECL90,0	11h46m01s	+01d11'25''	176.26°	-0.30°	+90.2°	39' x 39'

A/W of the P2 detector, and applying a preliminary correction of 0.55 for signal increase in the 180'' aperture with respect to the aperture for which the calibration of responsivity had been performed on standard stars (see Lemke 1997). Comparing the average surface brightness of our maps, listed in Table 2, with COBE/DIRBE weekly maps (see Boggess et al. 1992 and Silverberg et al. 1993) we found deviations of less than 10% (no colour correction has been applied to either data set).

Because long term detector drifts in ISOPHOT were anticipated, we also performed two cross scans on each map following the raster measurement. These short duration scans are less affected by drift, providing a possibility to correct the raster measurement by comparing directly sky positions observed both in the cross scans and in the map. Also linear gradients were removed from the map. After this process, the map looks like shown in Figure 1. Since the initial part of the drift in the raster measurement could not be well corrected for by our procedure, we omitted the pixels around the edge of the field, where the first measured pixels are situated, in the following analysis.

The fluctuation of surface brightness in the maps was determined by two independent methods. First, we plotted the histogram of pixels and fitted the central part of the distribution by a Gaussian (see Figure 2). The standard deviation of this fit is denoted in Table 2 as ‘Histogram, 1σ ’. As a second method, we calculated the structure function of the maps,

$$S(\Delta) = \langle |F(\mathbf{x}) - F(\mathbf{x} + \Delta)|^2 \rangle_{\mathbf{x}}$$

where, for a given separation Δ , the average is taken over all sky locations \mathbf{x} of the map, and in addition was performed over all position angles of the separation vector. We then estimated the fluctuation as $\sqrt{0.5}$ * the value of the structure function at 3' (see Figure 3). In general these two measures of noise agree. Table 2 lists the average surface brightness of the maps as well as the 1 sigma fluctuations in MJy/sr determined from the histogram and the structure function, respectively. We also included the instrumental measurement uncertainties, derived from the fluctuations between the individual brightness readings, as given by PIA. The last two columns give the fluctuation of the maps after subtracting this instrumental measurement uncertainty quadratically from the observed fluctuations. These columns constitute the primary result of our measurement.

3. Results and discussion

Not unexpectedly, the results of our measurements shown in Table 2 confirm the general smoothness of zodiacal light. However, we consider the average residual fluctuation of $\pm 0.2\%$

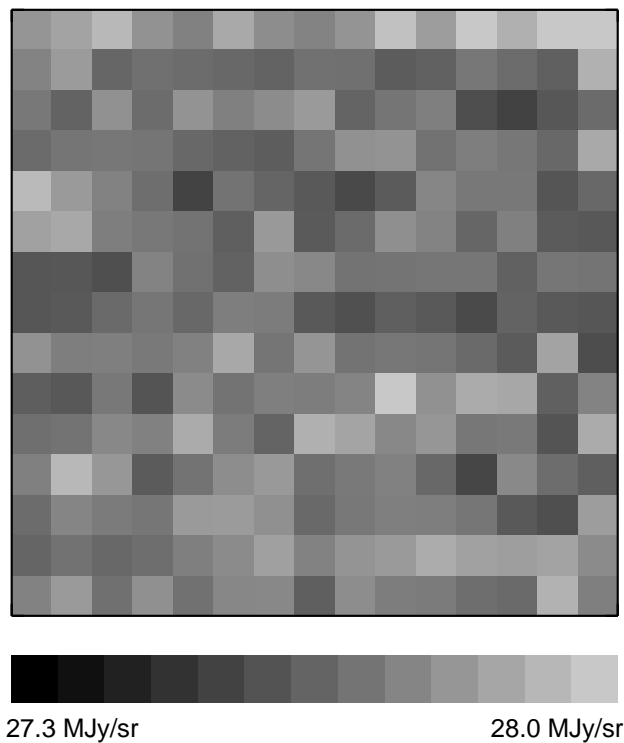


Fig. 1. Map of 45' x 45' obtained at the North Galactic Pole. The data have been drift-corrected as described in the text. Note that the map shows full 3' x 3' pixels for convenience only - the actual measurements were performed with a circular diaphragm of 3' diameter.

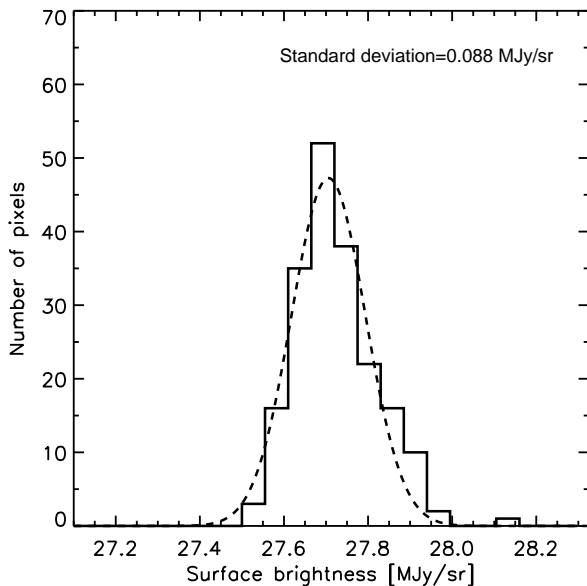
(± 25 mJy per beam at high ecliptic latitudes, ± 80 mJy in the ecliptic) only as an upper limit for possible true variations on 3' scales. First, we note that the absolute values of the fluctuations appear to increase with the total brightness in the field. This could be the signature of real zodiacal light fluctuations, but would also be the signature of variations in instrument sensitivity. Now, among the time series of the observations in the five fields at least one showed a clear event of a fluctuation in the detector sensitivity, as they typically occur after particle hits, corresponding on the sky to a quite untypical striplike depression. Therefore we assume that less conspicuous instrumental instabilities still contribute a significant amount to the observed fluctuations. Since at the level of fractions of a percent the instrument behaviour is not really known, we cannot quantify this contribution, and therefore take the full observed fluctuations as given in Table 2 as upper limits. This only emphasizes again the general smoothness of zodiacal light. Although the area cov-

Table 2. Instrumental noise and fluctuation of surface brightness [in MJy/sr]

Field Name	Mean surface brightness	PIA 1σ noise	From structure function	Histogram 1σ	Residual fluctuation ^{a,b}	
M01	23.76	0.034	0.087	0.052	0.039	0.17%
M02	23.32	0.043	0.067	0.044	0.009	0.04%
M03	23.43	0.035	0.067	0.051	0.037	0.16%
NGP	27.67	0.035	0.086	0.088	0.081	0.29%
ECL90,0	67.60	0.047	0.145	0.133	0.124	0.18%

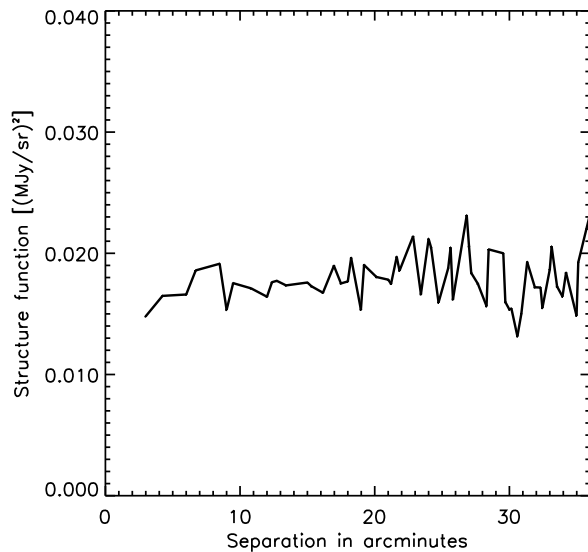
^a residual fluctuation (MJy/sr) = $\sqrt{\text{observed}^2 - (\text{PIA noise})^2}$ (where 'observed' refers to column 5)

^b residual fluctuation (%) = (residual fluctuation [MJy/sr])/(total surface brightness)

**Fig. 2.** Histogramm of the brightnesses measured in the central 13x13 pixels of the map at the North Galactic Pole.

ered is small (1.6 degree² or ≈ 640 individual measurements), we consider the result as representative and do not expect that larger samples to be accumulated during the ISO mission will lead to a different result.

We do not anticipate an important contribution to the observed fluctuations from other astronomical sources. The regions mapped were selected for low cirrus emission, ≈ 2 MJy/sr at 100 μm , which corresponds to 0.09 MJy/sr at 25 μm (Désert et al. 1990), and for which a brightness fluctuation of ≈ 0.001 MJy/sr is predicted for a 3' diameter field-of-view at 25 μm (Helou and Beichman 1990). This is well below the limits on brightness fluctuation derived from our measurement. Stars also were avoided in our fields, down to magnitudes of $R = 12$. Even a rather red star of this brightness, spectral type M4, with a typical colour index of $R-N \approx 4.5-5$, would have an estimated 25 μm flux of only 6-10 mJy (corresponding to 0.010 MJy/sr - 0.017 MJy/sr), again small compared to the measured fluctuations. Also, one or two sources from the IRAS faint source catalogue, with upper flux limits of between 40 mJy and 140 mJy, fall into our fields, but they are not causing a signal at their position which obviously exceeds the general level of fluctuation. Any-

**Fig. 3.** Structure function $\langle(I_i - I_j)^2\rangle$ calculated from the measured single-pixel brightnesses in the map at the North Galactic Pole. The smallest separation is the pixel separation of 3', the largest separation is determined by the size of the map.

way, the method of histogram fitting is not very sensitive to the existence of a few point sources in the field. The observed fluctuations therefore appear not to be due to background sources. Rather they have to be attributed, as assumed above, mostly to a combination of intrinsic zodiacal light brightness fluctuations and the present instrumental noise limit. Our values give upper limits to both of these effects.

As far as the zodiacal light is concerned, this relative smoothness of the brightness distribution does not mean that the cloud of interplanetary dust has to be homogeneous. Rather it emphasizes the efficiency of mixing to which the interplanetary dust is subject by gravitational, electromagnetic and mechanical forces. The few known structures in the zodiacal light are the exceptions from the rule: cometary trails and asteroidal bands show dust close to the locus of production respectively in a region of enhanced production, while the dust ring outside the earth's orbit (Dermott et al. 1994) is caused by a special, resonant interaction.

The observed limit on zodiacal light fluctuations has also to be considered for deep source counts, since such small-scale

fluctuations may degrade the detection limit or introduce systematic uncertainties. The structure function of the fluctuations shown in Figure 4 is flat, indicating a statistical behaviour like for white noise. We therefore assume that this is the behaviour of the fluctuations also at the smaller separations not observable in our data. The fluctuations then simply scale with the diameter of the aperture (pixel size), like in the photon noise limit. An extrapolation to other beam sizes is therefore not so problematic and can be extended to the longer wavelengths of 60 μm or 90 μm , where the Airy disks and the pixel sizes (at least for ISO) are still comparable to our diaphragm size. Using the average zodiacal light spectrum as measured by COBE at 90° from the sun in the ecliptic, and the pixel sizes of 45'' used on ISO, and assuming that the fluctuations are proportional to observed zodiacal light brightness, we then predict fluctuations of less than 2 mJy at 60 μm and smaller than 1 mJy at 90 μm . This is far below the cutoff of 50 mJy reached in the deep IRAS source counts at 60 μm (Hacking and Houck 1987). It indicates that the above limits on zodiacal light fluctuations should not compromise faint source counts going to ten times fainter brightness limits. Of course, there are usually more restrictive limits due to cirrus fluctuations or instrumental effects.

At the wavelengths short of 25 μm much smaller pixel sizes are used ($\leq 12''$ in the infrared camera ISOCAM onboard ISO). Nevertheless, we note for information and comparison that the above assumptions (flat power spectrum for the fluctuations, proportionality to total zodiacal light brightness) lead to an upper limit to 1σ fluctuations for a pixel size of 6'' of ± 0.06 mJy at 7 μm and ± 0.45 mJy at 15 μm .

4. Conclusions

Mapping five fields at different ecliptic latitudes we determined an upper limit on the observed brightness fluctuations of $\pm 0.2\%$ at 25 μm , corresponding to ± 25 mJy in the 3' beam at high ecliptic latitudes. This supports the concept of a generally smooth zodiacal light distribution. Faint source counts at brightness levels down to ≈ 5 mJy at 60 μm or 90 μm will not be affected by potential small-scale zodiacal light structures.

Acknowledgements. The ISOPHOT instrument was funded by the Deutsche Agentur für Raumfahrtangelegenheiten (DARA), the Max-Planck-Gesellschaft, and CoI-institutes in several European countries. Members of the ISOPHOT Data Center at MPIA Heidelberg and of the Instrument Dedicated Team at ESA/VILSPA, in particular U. Herbstmeier, supported us in data reduction and calibration. The ISOPHOT data presented in this paper was reduced using the ISOPHOT interactive analysis software "PIA", which is a joint development by the ESA Astrophysics Division and the ISOPHOT consortium led by the Max Planck Institute for Astronomy (MPIA), Heidelberg

References

- Boggess N. et al. 1992, ApJ 397, 420
 Dermott S.F., Jayaraman S., Xu Y.L., Gustafson B.Å.S. and Liou J.C. 1994, Nature 369, 719
 Désert F.-X., Boulanger F., and J.-L. Puget 1990, A&A 237, 215
 Hacking P. and Houck J.R. 1987, ApJ Suppl. 63, 311

- Helou G. and Beichman C.A. 1990, Proc. 29th Liège International Astrophysical Colloquium "From Ground-Based to Space-Borne Sub-mm Astronomy, ESA SP-314, p.117
 Lemke D. and 47 co-authors 1996, A&A 315, L64
 Lemke D. 1997, contribution in "Taking Iso to the limits: exploring the faintest sources in the infrared", ESA/ESTEC proceedings of a workshop in Villafranca in February 1997.
 Levasseur A.C. and Blamont J.E. 1973, Nature 246, 26
 Reach W.T. 1992, ApJ 392, 289
 Richter I., Leinert Ch., and Planck B. 1982, A&A 110, 115
 Silverberg R.F. et al. 1993, in Proc. SPIE Conf. 2019, "Infrared space-borne remote sensing", ed. M.S. Scholl, p.180
 Sykes M.V. 1990, Icarus 85, 267
 Sykes M.V. and Walker R.G. 1992, Icarus 95, 180